2) Photolithography

The mask patterning was performed by photolithography technique using TSMR 8900 as photoresist. Coating of photoresist over the sample surface was performed using a spin coater with two step rotation. Then the photoresist was pre-baked at 110 °C for 90 seconds before performing the exposure process to make waveguide patterns. The developing process after exposure was performed using NMD3 as developer. After that, the mask patterning was finished by post-baking at 130 °C for 3 minutes. The exposure time, developing time, and other photolithography conditions are summarized in Table 4.2.

Table 4.2 Photolithography condition

Parameters	*Condition*
Photoresist	TSMR 8900 Positive
Spin coating	
1st step speed/time	500 rpm / 5 sec
2nd step speed/time	6000 rpm / 40 sec
Prebaking	1:30 min
Expose time	3.7 sec
Develop time	25 sec
Postbaking	3:00 min

3) Etching of SiO_2 Mask

To make the etching mask, the SiO_2 was then etched using Inductively coupled plasma (ICP) etching technique. The ICP etching of the SiO_2 mask was carried out in a gas mixture of Ar (4 sccm), CHF_3 (7 sccm) and O_2 (0.3 sccm) under a reactor pressure of 1 Pa. The ICP power and bias power were maintained at 75 W and 30 W, respectively.

4) Removal of Photoresist

The photoresist that is left on the SiO_2 mask can be removed by ashing process with O_2 for about 5 minutes. To avoid damage occurred from ashing, Hakuri 106 was used to clean the left photoresist instead, which requires cleaning by boiled IPA in ultrasonic bath.

5) Waveguide Etching

The most important process to fabricate the waveguide is the etching of GaN and related materials such as AlGaN. In this research, the etching of such materials was carried out by ICP etching technique using Cl_2 plasma. The details concerning etching condition and optimization is discussed in the next section.

6) Removal of SiO_2 Mask

The next process after finishing the waveguide etching is to remove the SiO_2 that is left on the waveguide. This can be performed by using SiO_2 etching recipe as mentioned in *3)*. However, to avoid the deterioration of the waveguides, removal of SiO_2 mask was carried out by wet etching using buffer HF as etchant.

7) Cleaving

The final process to make the waveguides is the cleaving process. The waveguide must be cleaved to get good facets in order to couple the laser light from tapered fiber. However, the thickness of the substrate after finishing all etching process is still too

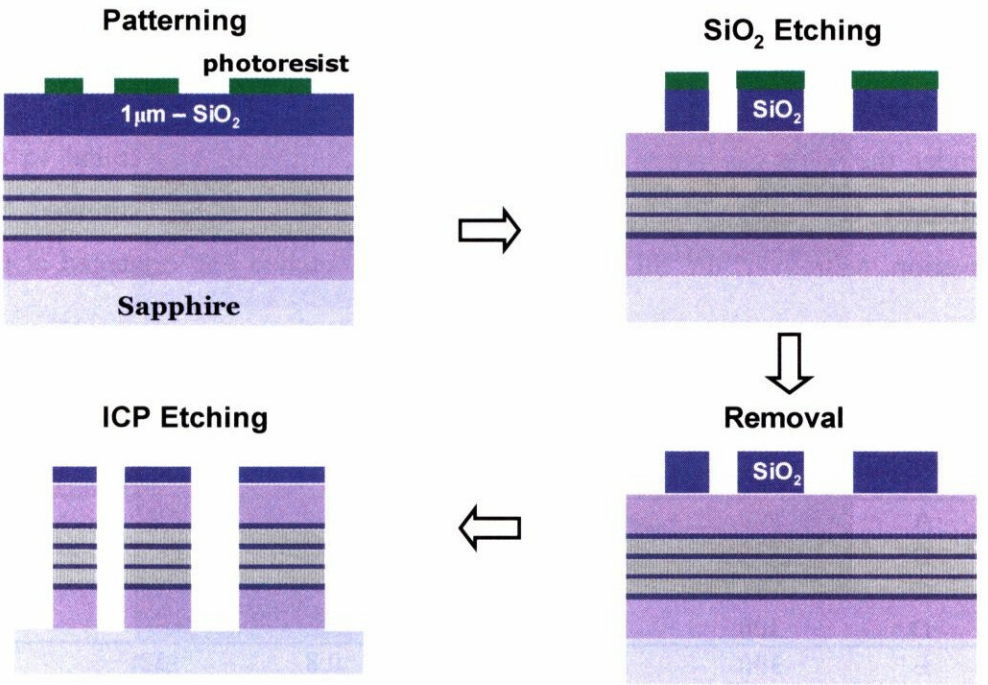

Figure 4.9 Schematic diagram of waveguide fabrication process

thick since the thickness of sapphire substrate is 330 μm, making it very difficult to be cleaved for high quality facets. The waveguide wafer is therefore necessary to be polished to obtain a wafer thickness of around 100 μm, followed by polishing the lapping surface to obtain mirror-like surface. With this thickness, the cleaving can be easily performed along the *a*-plane of sapphire substrate using a scriber machine.

4.2.2 Optimization of GaN etching [169]

In this study, etching of GaN was performed by inductively coupled plasma (ICP) etching using gas mixture of Cl_2 and Ar under a total flow rate of 10 sccm. To find the optimal condition for GaN etching, the gas pressure, gas mixing ratio, ICP power and bias power were varied with condition shown in Table 4.3 to study their influences on the etched sidewall profiles, surface morphologies, etching rates and selectivities of the GaN layer to the SiO_2 mask. Scanning electron microscope (SEM) and Atomic force microscope (AFM) were used for the observation of the cross sectional images and surface morphologies of samples.

At first, the influence of the gas pressure under a fixed ICP power and a bias power was investigated. For the condition that only Cl_2 was used without mixing of Ar, the etching rate of GaN clearly decreased and the etched sidewall became anisotropic with increasing Cl_2 pressure. The etching rate of the SiO_2 mask, on the other hand, increases with Cl_2 pressure, resulting in a decrease in selectivity of GaN to SiO_2 mask.

Under the high gas pressure of 10 Pa, the etching rate was found to decrease significantly to a very low etching rate, which could not be estimated by SEM observation. Moreover, the SiO_2 mask was severely etched and damaged at this high

Table 4.3 Etching conditions and results for optimization

Sample	ICP power (W)	Bias power (W)	Pressure (Pa)	Cl2 content	Etching rate (nm/min)	Etching selectivity
A	300	150	5	1	200	5
B	300	150	7	1	167	4
C	300	150	9	1	130	3
D	300	150	10	1	—	—
E	300	175	7	0.8	152	10
F	300	200	7	0.8	220	9
G	250	175	7	0.8	113	7

pressure. In general, at a higher pressure environment, the collisional scattering rate of the ions becomes higher, and the self-bias of the wafer stage becomes lower, resulting in the weakening of the effect of ion bombardment on the surface of etching sample. Considering these results, a low Cl_2 pressure is clearly preferable for enhancing isotropic GaN etching and suppressing the damage of the SiO_2 mask. It is also found that the etching of GaN is significantly dependent on the effect of ion bombardment, which can be enhanced by introducing Ar to the system. At the lowest pressure of 5 Pa, although the etching rate was the largest, the effect of ion bombardment was so strong that the abruptness of the sidewall was degraded due to the erosion of the masks. The gas pressure was therefore fixed at 7 Pa while changing the other parameters for further investigation.

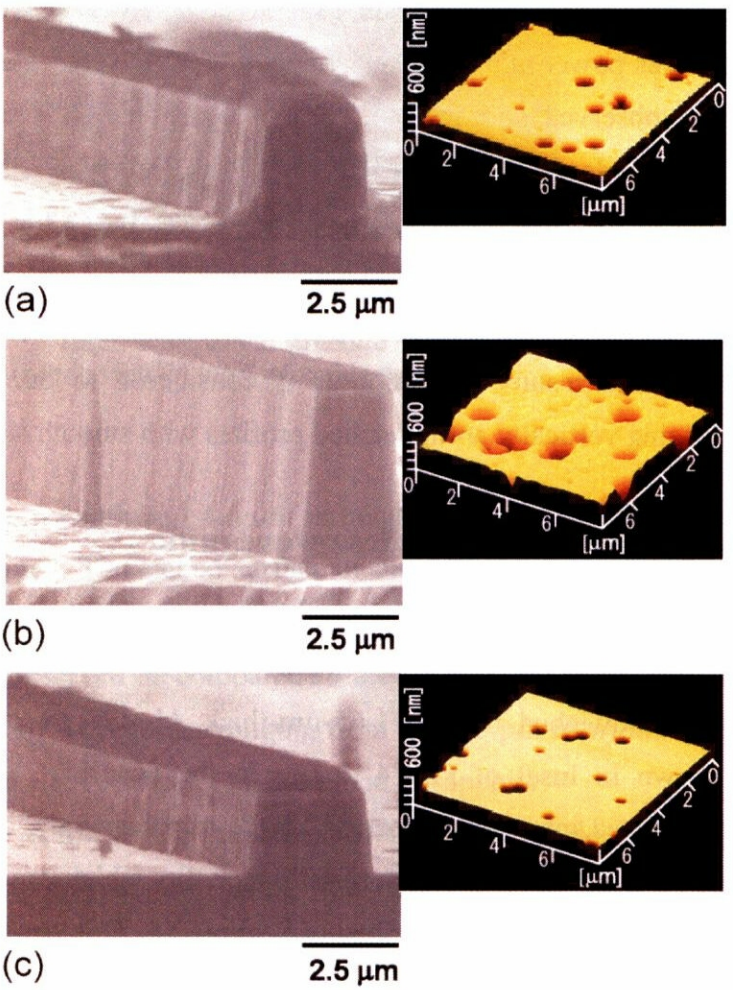

Figure 4.10 Cross sectional SEM images and AFM surface morphologies of samples etched with different conditions: (a) condition E, (b) condition F, (c) condition G

Next to the optimal etching pressure, the influences of the ICP power and bias power for conditions E, F and G as shown in Table 4.3 are investigated. The results of the SEM images and AFM surface morphologies are also shown in Fig. 4.10. The increase in bias power to 175 W improved the selectivity to 10, which is higher than those previously reported in literature [170]. Additionally, the SEM observation revealed that the sidewall of this sample was smooth with a better vertical profile as expected (Fig. 4.10 (a)). However, though the etching rate increased, a further increase in bias power to 200W led to a decrease in the selectivity and also deterioration of the sidewall. With this high selectivity, the vertical stripes observed on the sidewall of waveguides are thought to be a reflection of the SiO_2 mask morphology, indicating that the SiO_2 mask patterning process strongly affects the results of the subsequent GaN etching.

In order to realize smoother sidewalls, the ICP power was reduced from 300 W to 250 W under the bias power of 175 W. As shown in Fig. 4.10 (c), however, no marked improvement was observed and instead, the abruptness and the etching selectivity deteriorated due to the lower plasma density. The AFM images of the figures suggest that the roughness of the etched surface is not simply related to the ICP power or the bias power. The RMS values of the etched surfaces (44.9, 123.7 and 31.2 nm) are large, but these rough surfaces do not severely influence the light propagation in the waveguide. With these results, condition E is considered to be the most optimal condition for realizing vertically abrupt etched profiles with smooth sidewalls.

4.2.3 Fabrication of GaN high-mesa waveguide

Using optimal etching condition found in the last section, a high-mesa waveguide was fabricated. The waveguide structure consisting of 40-period AlN(1.6 nm)/GaN(1.6 nm) MQW core part, sandwiched by two 1.65-μm-thick $Al_{0.1}Ga_{0.9}N$ cladding layers, as schematically shown in Inset of Fig. 4.11 (a). In the core part, 0.4-μm-thick GaN interlayers were inserted into each 10-period MQW to enhance the effective refractive index of the core part, and to restore the crystalline quality which can be deteriorated by growing too thick MQW layers as described in Section 2.4. This structure was designed to achieve sufficient optical confinement into the core part at a wavelength of 1.55 μm.

As shown in the cross sectional SEM image of Fig. 4.11 (a), the high-mesa

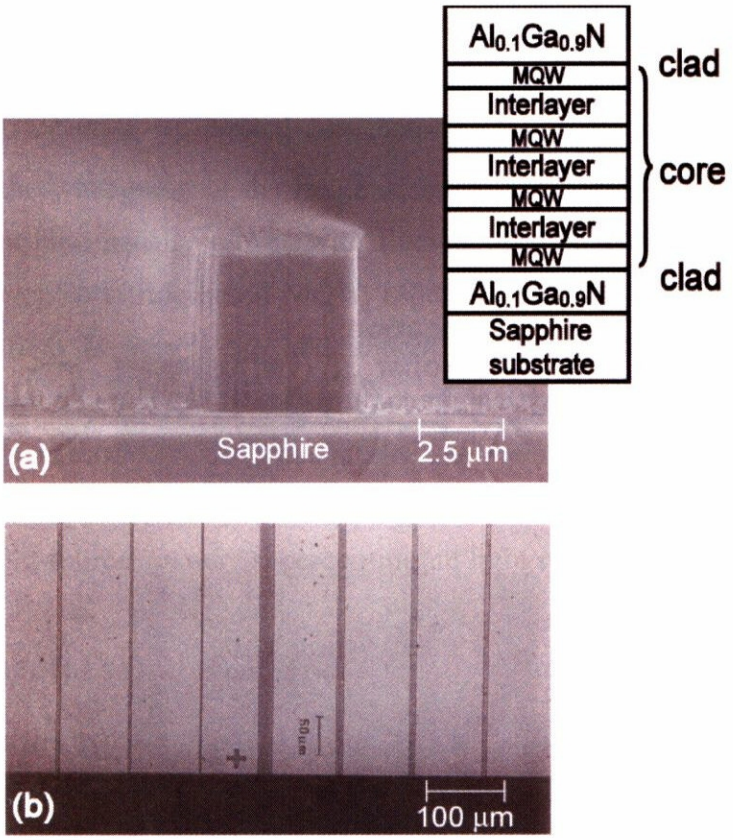

Figure 4.11 (a) Cross sectional SEM image of as-fabricated high-mesa waveguide. Inset: schematical structure of the waveguide.
(b) top view of the waveguide wafer.

waveguide (4 μm in width and 4.6 μm in height) with a vertically abrupt sidewall was successfully obtained. The etched surface of the $Al_{0.1}Ga_{0.9}N$ layer was nearly similar to that of the GaN layer using the same etching condition, and no remarkable change in etching rate was observed as compared to the GaN layer. Figure 4.11 (b) shows a top view of the series of waveguides ranging from 2 to 20 μm in width. The bottom surface of the figure is the cleaved facet, (11-20) plane of sapphire.

In order to confirm the function of the waveguide, the light propagation experiments were carried out using the fabricated high-mesa waveguides. The experimental setup includes the 1.55 μm laser as a light source, polarization controller, tapered fiber, optical power meter, and infrared camera, as shown in Fig. 4.12 (a). The 1.55 μm laser light was carefully coupled to the waveguides, then the light propagation

in the waveguides was confirmed by using an infrared camera. Figure 4.12 (b) shows the near-field image of the light propagation through the waveguide. As can be seen in the figure, round beam of propagated light is clearly observed, indicating that the waveguide was successfully fabricated and it can be used for the realization of nitride-based optical devices.

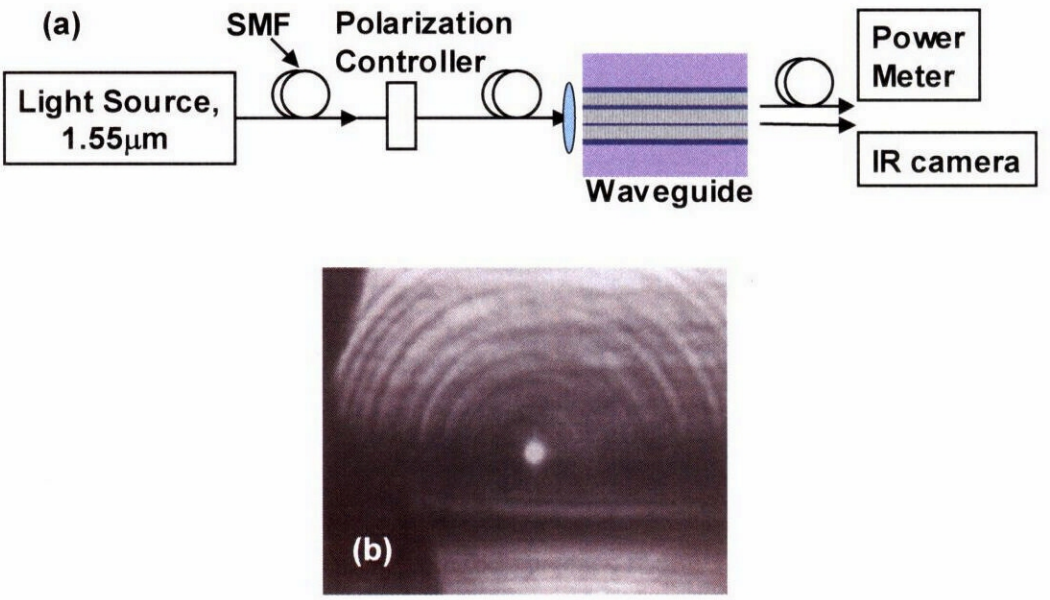

Figure 4.12 (a) Waveguide measurement Setup
(b) near-field image of propagated light at 1.55 μm

4.3 Characterization of Waveguides by Supercontinuum Light Source

The characterization of the passive optical waveguide is the fundamental step for the design and fabrication of photonic devices. This process is also important to improve the processing technology by giving feedback from the characterization results. In this study, the measurements are therefore performed for many different kinds of waveguides. The parameters that we are important to characterize in this study are propagation loss, fiber-to-waveguide coupling loss, and polarization dependence. There are various well-known methods to measure the optical propagation loss and

fiber-to-waveguide coupling loss. Two main methods which have been used for the characterization of the passive waveguides are Fabry-Perot Resonance method and Cut-back method. The waveguide that contains intersubband absorption, however, have a wide range of absorption. These two methods, therefore, cannot be used to find the characteristic of the waveguide in the range of interest. Generally, the wavelength of intersubband absorption usually moves with fluctuation of thickness in quantum well structures. Moreover, in nitride-based MQW, especially GaN/AlN MQW, the effect of internal electric field is very large and almost uncontrollable, the wavelength of intersubband absorption moves even larger unintentionally. Therefore, there should be a new measurement method that can characterize the waveguide in the wide range of measurements. In this study, a new waveguide characterization method, using ultra-wideband light source, namely supercontinuum light source, has been developed.

4.3.1 Experimental setup

Figure 4.13 shows the experimental set up for the intersubband absorption measurement by waveguide coupling method. The light from ultra-wideband light-source is coupled to waveguides by tapered fiber, while the light came out of the waveguide was focused to a small point using 100X lens at the other side of the waveguides. The light propagated through the waveguide was coupled to a large-diameter fiber using collimating lens, making it ready for measurements by Power meter and Optical Spectrum Analyzer, etc. A small pin-hole was used to filter only the light that propagated through the waveguide, so that the filtered light was coupled to the fiber with less noise. Since the ultra-wideband light-source typically generates non-polarized

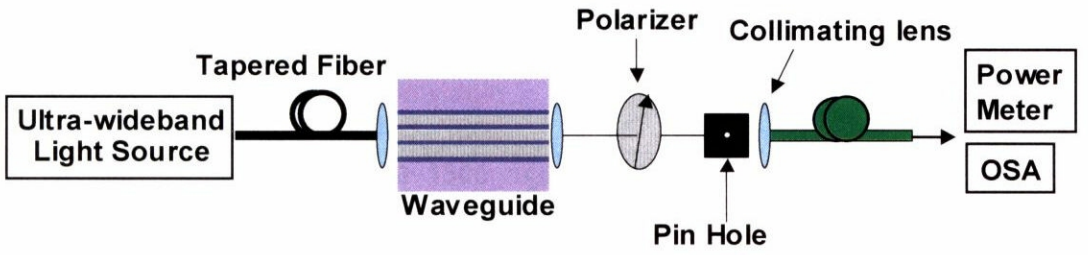

Figure 4.13 Measurement Setup of waveguide characterization using supercontinuum light source.

light, the polarization of light propagated through the waveguides was filtered and selected by putting a polarizer on the light path from waveguide to the collimating lens. This polarizer can be rotated to get the maximum output for TE mode or TM mode, with distinction ratio of higher than 20 dB. Finally, the transmission spectra for both TE and TM mode light can be taken by the Optical Spectrum Analyzer, and with the selection rule that intersubband absorption absorbs only TM mode light, the absorption spectra can be calculated by finding the ratio of TM mode transmitted power to TE mode transmitted power, or just subtracting the difference of powers in logged scale.

4.3.2 Supercontinuum light source

The conventional wideband light sources that are commercially available usually give a wavelength range not over than 200 nanometers centered at 1.55 μm, optical telecommunication wavelength. The halogen lamp is widely known for its ultrawide wavelength range, but the high power light cannot be obtained when coupling the light to single-mode optical fiber, which is necessary in the waveguide measurements. Recently, some new light sources that are able to couple to optical fiber and have wide wavelength range have therefore been developed [148-155].

One of the best techniques to produce the supercontinuum light source is to use the

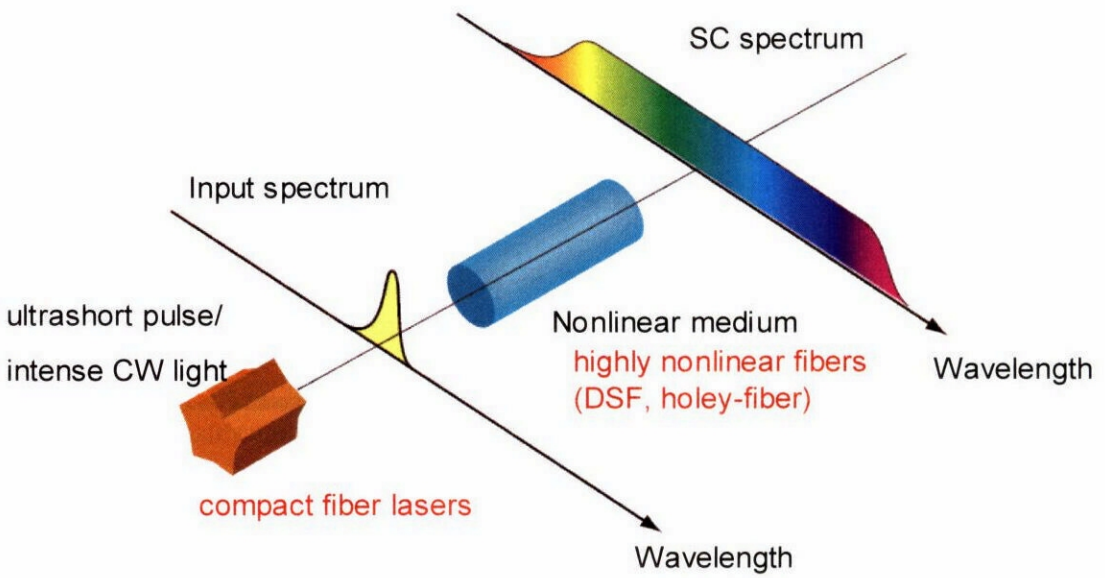

Figure 4.14 Schematic diagram of supercontinuum light generation

nonlinearity effect in the optical fiber [149-152], as illustrated in Fig. 4.14. When an ultra-short pulse is sent through highly nonlinear optical fiber, the light interacts with the fiber in a nonlinear fashion, converting the single-colored laser light into a broad spectrum of colors. Recently, there is another technique to produce the wideband light source using noise-like pulse mode [148]. It has been shown that long-cavity fiber lasers composed of low birefringent fibers could produce a noise-like pulse train, in which sub-picosecond pulses were gathered within a several tens picosecond envelope. The important feature of the noise-like pulse is its broad, smooth spectrum, which is free from the spectrum ripple seen in soliton lasers [171]. In this study, the broadband noise-like pulse was generated by using an EDF laser [155]. The output light from the supercontinuum light source used in this study has very wide band spectrum from 1100 nm to 1750 nm and high power, as shown in Fig. 4.15. Note that long wavelength side is expected to be as long as 2200 nm, but the measurement is limited by the upper wavelength range of spectrum analyzer at 1750 nm. This spectrum covers 1550 nm, the optical fiber communication wavelength, indicating that it can be used for characterization of waveguides, including intersubband absorption measurements.

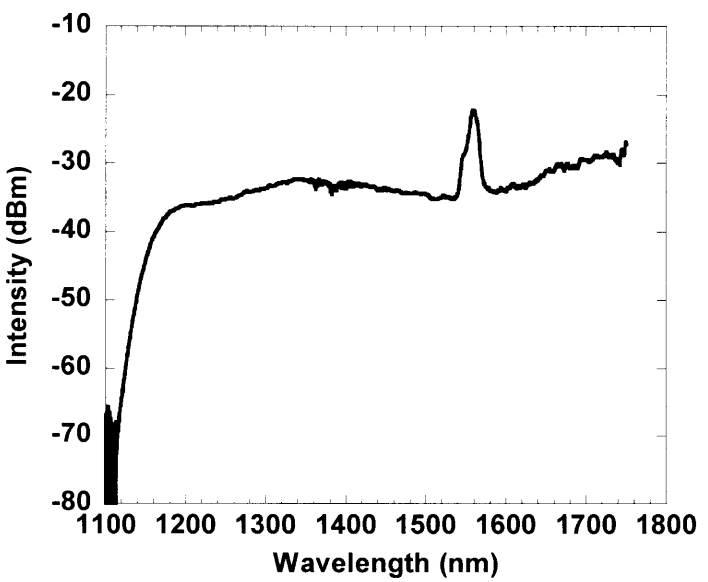

Figure 4.15 Spectrum of supercontinuum light source

4.3.3 Characterization of waveguides

To study the waveguide characteristics, the waveguides were characterized by the waveguide coupling method using the supercontinuum light source. Three kinds of waveguides investigated in this study are different by the growth technique that is used to grow the waveguide structures as summarized in Table 4.4.

Table 4.4 Growth methods of waveguide structure for characterization

Sample	Growth method		
	Bottom GaN clad	MQW	Upper GaN clad
A	MOVPE	MOVPE	MOVPE
B	MBE	MBE	MBE
C	MOVPE	MBE	MBE

Since the characterization by supercontinuum light source can measure the transmission spectra of TM-mode and TE-mode light separately with wide wavelength range, the difference between TM and TE mode can be used to determine the intersubband absorption wavelength and also the polarization dependence. In general, nitride-based semiconductors have defects, namely threading dislocation, in their crystal because mostly lattice-mismatched substrates such as sapphire are used. This kind of defects are essentially generated by lattice mismatch between GaN and sapphire substrate, usually used as a substrate in growing nitride-based semiconductors as until now it is still difficult to obtain a high-quality GaN substrate. The defects could make the crystalline quality becoming worse. Moreover, the threading dislocation generally spread along the growth direction, causing the optical transmission loss for the light in which its electric field component is parallel to the defects, that is, TM-mode light. In nitride semiconductors, the TM mode light therefore always has higher propagation loss than the TE mode light.

Figure 4.16 (a) shows TM and TE mode transmission spectra of Waveguide A, which was totally grown by MOVPE technique. This waveguide has no absorption in the range of measurements confirmed by the multiple-reflection method. The ideal

transmission spectra should therefore show no difference between TM and TE mode. The difference in transmission spectra between the TM and TE mode (TM-TE) can be calculated as shown in Fig. 4.16 (b). As can be seen in the figure, there is almost no difference in transmission spectra between TM and TE mode, with only some little noise observed. This indicates that the crystalline quality of the MOVPE-grown waveguides is very good, with no additional loss observed for TM mode light.

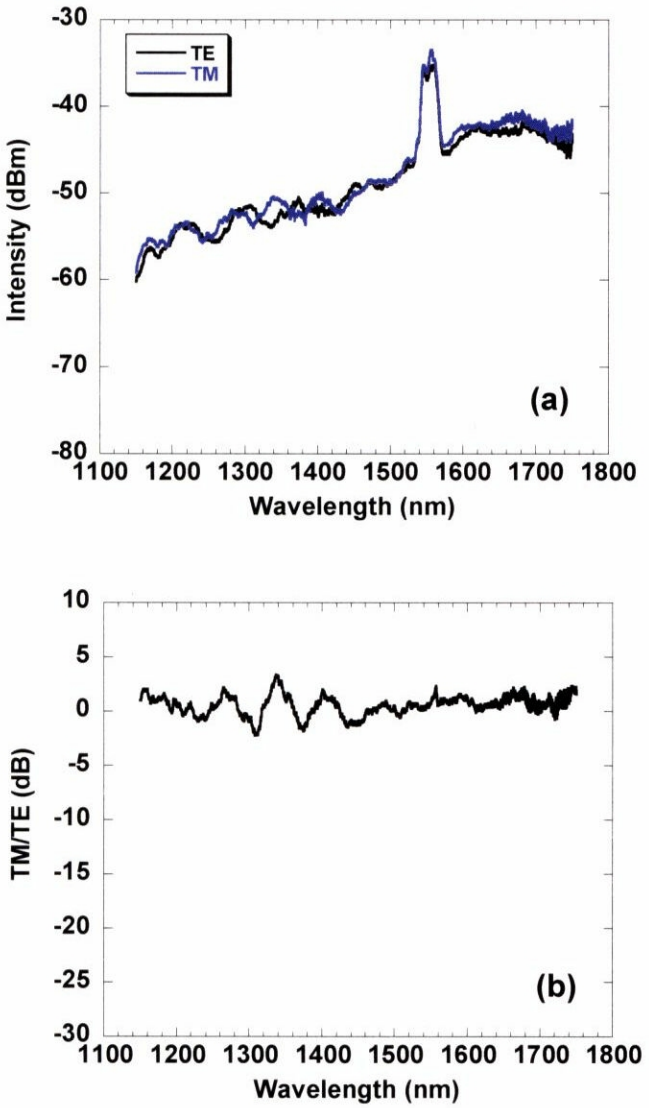

Figure 4.16 (a) TM and TE mode transmission spectra waveguide A
(b) TM/TE ratio of waveguide A

Figure 4.17 (a) shows TM and TE mode transmission spectra of Waveguide B, which was totally grown by MBE technique. The intersubband absorption measurement by multiple-reflection method has shown that this waveguide has intersubband absorption with peak wavelength of 1.75 μm, as measured for a specimen fabricated from the same wafer as Waveguide B. Note that periodic noise observed in both TM and TE mode is a result of multi-mode transmission inside the waveguides as the coupling of fiber-waveguide could generate many modes of propagation especially for the waveguide structure that is not optimized for single-mode transmission. Although the

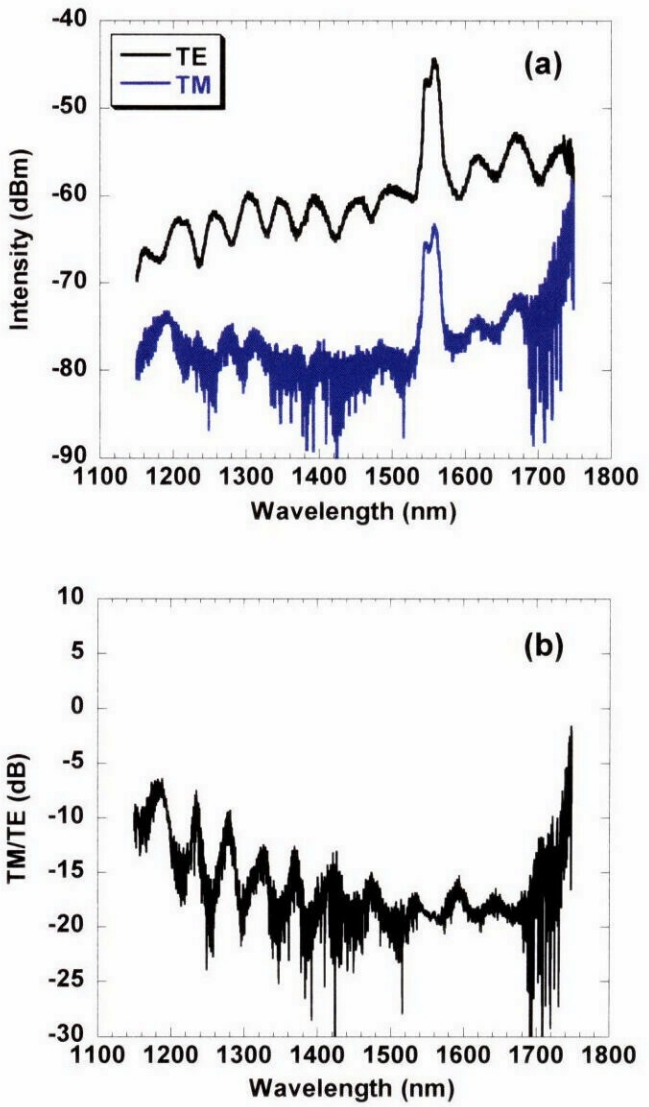

Figure 4.17 (a) TM and TE mode transmission spectra waveguide B
(b) TM/TE ratio of waveguide B

transmission spectra are interfered by the multi-mode transmission, the transmission spectra show big difference in the intensity of transmitted light between TM and TE mode. Even in the wavelength range that the effect of intersubband absorption should not be observed, for example in the range of 1.1-1.2 μm, the polarization dependence is clearly observed. Such difference between the TM and TE mode as shown in Fig. 4.17(b) reveals that the waveguides generate additional loss for TM mode transmission of approximately 10 dB in intensity, excluding the loss occurred by intersubband absorption. This additional TM mode loss is therefore considered to be caused by crystalline defects of the MBE-grown waveguide structures. Even though some growth techniques, such as GaN/AlN superlattice buffer layer [137], were applied to get good crystalline quality by MBE growth technique, the crystalline quality obtained is still not good enough for the fabrication of high-quality waveguides. With comparison between Waveguide A and Waveguide B, it can be considered that the MOVPE growth is much better than MBE growth in order to get good crystalline quality. However, the wavelength of intersubband absorption is still a main problem in making the devices for intersubband transition.

Figure 4.18 (a) shows TM and TE mode transmission spectra of Waveguide C, which the thick GaN buffer layer were firstly grown by MOVPE technique, whereas the MQW and GaN upper layer were subsequently grown by MBE technique. Since both Waveguide C and Waveguide D contains only two quantum wells, the intersubband absorptions are very weak, and not detectable with measurements by Multiple-reflection method. The difference between TM and TE mode for both waveguides was also plotted, as shown Fig. 4.18 (b). As can be seen in the figure, the intersubband absorption can be observed with the measurements by waveguide-coupling method. There is big difference in intensity between TM and TE mode at a wavelength of around 1.7 μm, while the difference gradually decays to almost zero at shorter wavelength. These results show that intersubband absorption peak wavelength should be at 1.7 μm. For shorter wavelength of around 1.2 μm, there is almost no difference in transmission intensity between TM and TE mode, which means no additional TM mode transmission loss is observed. This indicates that the crystalline quality of the MOVPE-grown buffer layer is still good even though it is stacked by MQW and GaN layer that are grown by the MBE growth technique.

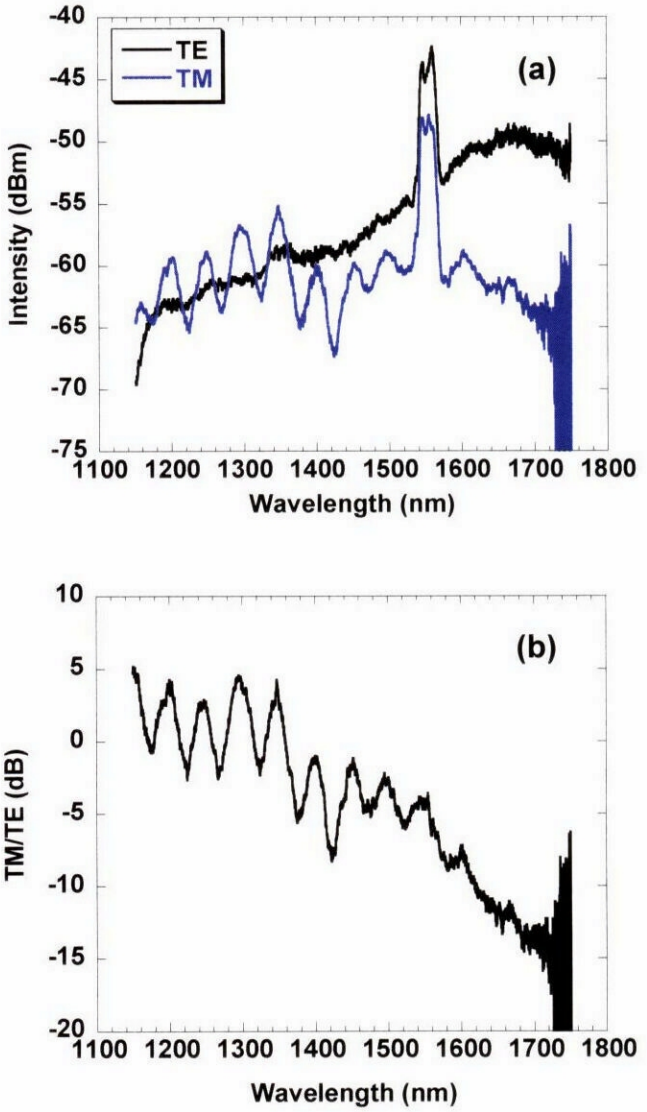

Figure 4.18 (a) TM and TE mode transmission spectra waveguide C
(b) TM/TE ratio of waveguide C

Considering these results, the combination of MOVPE growth and MBE growth is a practical solution to get good crystalline quality while still keeps ability to control the wavelength of intersubband transition which can be achieved at any desired wavelength, especially the optical communication wavelength range of 1.3-1.55 μm.

4.4 Concluding Remarks

In this chapter, the fabrication and characterization of GaN-based waveguide structures were studied. Firstly, several waveguide structures were proposed and investigated for their possibilities to use as a waveguide structure for the intersubband transition device. It was found that for GaN waveguide, the total thickness have to be thinner than 800 nm to maintain the single-mode propagation. To obtain a high-optical-confinement waveguide structure, the structure requires a low refractive index material, such as AlGaN or AlN to use as cladding layers.

In Section 4.2, the GaN waveguide structure was fabricated and characterized. The fabrication of GaN waveguide was successfully demonstrated by the inductively coupled plasma etching technique. The optimal etching condition was found out: flow rate of Cl_2/Ar: 8/2, pressure: 7 Pa, ICP power: 300 W, bias power: 175 W.

In Section 4.3, the new waveguide characterization method, using supercontinuum light source, was proposed and demonstrated for the first time. This characterization method has clarified that the waveguide structure grown by metalorganic vapor phase epitaxy has very good crystalline quality suitable for the fabrication of intersubband transition devices. On the other hand, the waveguide structure grown by molecular beam epitaxy provides a high propagation loss for TM-polarization owing to a high density of crystalline defects in the structure. It was thus found that in order to fabricate a high-quality waveguide of nitride-based semiconductors, not only the waveguide fabrication process, but also the epitaxial growth of the waveguide structure requires a careful concern of each step to obtain the best quality.

For the growth of thick high-quality epilayer, the metalorganic vapor phase epitaxy is therefore preferable, while the molecular beam epitaxy is also needed for the growth of multiple quantum well structures with intersubband absorption at 1.55 μm. In order to realize the nitride-based intersubband transition devices, a combination of both the metalorganic vapor phase epitaxy and molecular beam epitaxy is therefore a solution to achieve the high-quality waveguides with desired intersubband absorption.